PUBLISHED VERSION

http://link.aps.org/doi/10.1103/PhysRevC.75.045202

http://hdl.handle.net/2440/44809

Phase transition from hadronic matter to quark matter

P. Wang,[1,3] A. W. Thomas,[2] and A. G. Williams[3]

[1]*Physics Department, North Carolina State University, Raleigh, North Carolina 27695, USA*
[2]*Jefferson Laboratory, 12000 Jefferson Ave., Newport News, Virginia 23606, USA*
[3]*Special Research Center for the Subatomic Structure of Matter (CSSM) and*
Department of Physics, University of Adelaide, Adelaide, SA 5005, Australia
(Received 22 October 2006; published 9 April 2007)

We study the phase transition from two-flavor nuclear matter to quark matter. A mean field model, constructed at the quark level, is used to give the equation of state for nuclear matter, while the equation of state for color superconducting quark matter is calculated within the NJL model. It is found that at low temperature, the phase transition from nuclear to color superconducting quark matter will take place when the density is of order $2.5\rho_0$–$5\rho_0$. At zero density, the quark phase will appear when the temperature is larger than about 148 MeV. Within the mean field treatment, the phase transition from nuclear matter to quark matter is always first order, whereas the transition between color superconducting quark matter and normal quark matter is second order.

I. INTRODUCTION

Hadronic matter is expected to undergo a phase transition to quark matter at high temperature and/or high baryon density. Quark matter may exist in the core of neutron star where the density is high or it may be produced in the laboratory in heavy ion collisions. In quark matter, the presence of a weak attraction between the quarks will result in the formation of a condensate of quark pairs. Pairs of quarks cannot be color singlets, and in QCD with two flavors of massless quarks, the Cooper pairs favor the formation of a color $\bar{3}$, flavor singlet condensate. The color superconductivity of quark matter has been discussed in many places in the literature (see, for example, [1–4] and references therein).

The phase diagram for chiral symmetry restoration, including possible color superconductivity, for quark matter containing just u and d quarks, was discussed in Refs. [5,6], where a rich phase structure was obtained. It was shown that at high temperature, chiral symmetry was restored via a second-order phase transition. At low temperature, the phase transition was first order and at this time, a new phase with a condensate of Cooper pairs appeared. However, we should notice that this phase transition is not a transition from hadronic matter to quark matter but a transition from chiral symmetry breaking quark matter to chiral symmetry restored quark matter. We know that in the real world, there is no quark matter at low density and temperature, rather the chiral symmetry breaking quark matter should be replaced by hadronic matter. Therefore, when studying the phase diagram, the equations of state (EOS) of hadronic matter are needed.

To study the properties of hadronic matter we need phenomenological models, since QCD cannot yet be used directly. The symmetries of QCD can be used to constrain the hadronic interactions and models based on $SU(2)_L \times SU(2)_R$ symmetry and scale invariance have been proposed. These effective models have been widely used to investigate nuclear matter and finite nuclei, both at zero and at finite temperature [7–9]. Papazoglou *et al.* extended the chiral effective models to $SU(3)_L \times SU(3)_R$, including the baryon octet [10,11].

As well as models based on hadronic degrees of freedom, there are others based on quark degrees of freedom, such as the quark meson coupling model [12,13], the cloudy bag model [14], the Nambu-Jona-Lasinio (NJL) model [15] and the quark mean field model [16], etc. Several years ago, a chiral $SU(3)$ quark mean field model based on quark degrees of freedom was proposed by Wang *et al.* [17,18]. In this model, quarks are confined in the baryons by an effective potential. The quark-meson interaction and meson self-interaction are based on $SU(3)$ chiral symmetry. Through the mechanism of spontaneous symmetry breaking the resulting constituent quarks and mesons (except for the pseudoscalars) obtain masses. The introduction of an explicit symmetry breaking term in the meson self-interaction generates the masses of the pseudoscalar mesons, which satisfy the relevant PCAC relations. The explicit symmetry breaking term in the quark-meson interaction gives reasonable hyperon potentials in hadronic matter. This chiral $SU(3)$ quark mean field model has been applied to investigate nuclear matter [19], strange hadronic matter [17], finite nuclei, hypernuclei [18], and quark matter [20]. Recently, we improved the chiral $SU(3)$ quark mean field model by using a microscopically justified treatment of the center of mass correction [21]. This new treatment has been applied to the study of the liquid-gas phase transition of asymmetric nuclear matter as well as strange hadronic matter [22,23]. By and large the results are in reasonable agreement with existing experimental data.

As we know, the phase transition between hadronic matter and quark matter can only occur at high density or temperature. As the density grows, one expects that the nucleons will begin to overlap. This is expected to be a source of short distance repulsion and correlations. Such effects are also encountered in atomic physics and a method of estimating the effect was introduced in Ref. [24]. This was later applied in the context of dense nuclear matter by [25] and we also use this method to estimate the importance of the effect. As we will show later, this procedure generates a repulsive interaction between the nucleons and increases their chemical potentials in nuclear matter.

In this paper, we study the phase transition from nuclear matter to quark matter. The effect of nucleon finite size is considered in nuclear matter and color superconductivity is discussed in quark matter. Since this is the first time we study the volume effect on the phase transition in our model, we restrict our investigation to just two flavors, without including strange quarks or hyperons. The paper is organized in the following way. Section II sets out the formalism of the NJL model which is applied to describe quark matter. In Sec. III we introduce the $SU(3)$ quark mean field model which is used to describe nuclear matter—although in this work only the nonstrange sector of the model is required. The effect of finite nucleon size is discussed in this section. The numerical results are presented in Sec. IV. Section V is the summary.

II. NJL MODEL

In order to study the color superconductivity of quark matter, we choose the NJL model, within which it is simple to incorporate the diquark condensate in the Lagrangian. The Lagrangian density for the $SU(2)$ NJL model [26] can be written as

$$\mathcal{L}_1 = \bar{\psi}_\alpha^i (i\gamma^\mu \partial_\mu - M)\psi_i^\alpha + G_1 \big[\bar{\psi}_\alpha^i \psi_i^\alpha \bar{\psi}_\beta^j \psi_j^\beta \\ - \bar{\psi}_\alpha^i \gamma_5 (\tau_a)_i^j \psi_j^\alpha \bar{\psi}_\beta^k \gamma_5 (\tau_a)_k^l \psi_l^\beta \big] - B', \quad (1)$$

where M is the current mass matrix of the u and d quarks, τ_a ($a = 1 - 3$) are the Pauli matrices. B' is the parameter which will give a reasonable bag constant, B, in quark matter. In order to describe the diquark condensate, the interaction of the color $\bar{3}$ fermion bilinears should be added. This four-fermion interaction can be written as

$$\mathcal{L}_2 = G_2 \big[(\bar{\psi}^T)_\beta^i C\gamma^5 \varepsilon^{\alpha\beta\gamma} \varepsilon_{ij} \bar{\psi}_\gamma^j \big](\psi^T)_\rho^k C\gamma^5 \varepsilon^{\alpha\rho\sigma} \varepsilon_{kl} \psi_\sigma^l, \quad (2)$$

where C denotes the charge conjugation matrix. In the above equations, G_1 and G_2 are the coupling constants.

From the above Lagrangian, the thermodynamic potential Ω, which determines the field equations can be obtained. It is convenience to introduce bosonic collective fields into the functional integral to make the four fermion interaction into a fermion-boson coupling. We follow Ref. [5] to employ a Hubbard-Stratonovich transformation, in which the collective fields are introduced into the functional integral by inserting the following identities:

$$1 = N_1 \int D\phi_q \exp\left\{ i \int \frac{d^4p}{(2\pi)^4} \left(\frac{\phi_q}{2} - G_1 \bar{\psi}_\alpha^i \psi_i^\alpha \right) \right. \\ \left. \times \frac{1}{G_1} \left(\frac{\phi_q}{2} - G_1 \bar{\psi}_\alpha^i \psi_i^\alpha \right) \right\}, \quad (3)$$

$$1 = N_2 \int D\Delta_q^* D\Delta_q \exp\left\{ i \int \frac{d^4p}{(2\pi)^4} \right. \\ \times \left(\frac{\Delta_q^{*\alpha}}{2} - G_2 \big[(\bar{\psi}^T)_\beta^i C\gamma^5 \varepsilon^{\alpha\beta\gamma} \varepsilon_{ij} \bar{\psi}_\gamma^j \big] \right) \\ \left. \times \frac{1}{G_2} \left(\frac{\Delta_q^\alpha}{2} - G_2 (\psi^T)_\beta^i C\gamma^5 \varepsilon^{\alpha\beta\gamma} \varepsilon_{ij} \psi_\gamma^j \right) \right\}. \quad (4)$$

The quadratic terms in Eqs. (3) and (4) cancel the original four-fermion interaction. As a result, the four-fermion interaction is cast into a Yukawa interaction between fermions and collective fields and a mass term for the collective fields. The fermionic fields then appear only quadratically and can be integrated out exactly, leaving an effective action for the bosonic collective fields alone. Having done the Gaussian integral for the fermions, the thermodynamic potential Ω_q reads

$$\Omega_q[\phi_q, \Delta_q; T, \mu] = \frac{1}{4G_1}\phi_q^2 + \frac{1}{4G_2}\Delta_q^2 + B' + \frac{i}{2}\ln\det \begin{pmatrix} \gamma^\mu p_\mu + \gamma^0 \mu_q - (m_q + \phi_q) & \Delta_q \\ \Delta_q^* & [\gamma^\mu p_\mu + \gamma^0 \mu_0 - (m_q + \phi_q)]^T \end{pmatrix}. \quad (5)$$

Disregarding the γ matrix, the matrix of the last term of the above equation is 12×12. Δ_q is a 6×6 matrix whose matrix elements are $(\Delta_q)^{i\alpha,j\beta} = C\gamma^5 \Delta_q \varepsilon_{ij} \varepsilon^{3\alpha\beta}$, where i, j are flavor indices and α, β are color indices.

The thermodynamic potential can be obtained by using imaginary time Green function method, with $p_0 = (2n + 1)\pi/\beta$ ($\beta = 1/T$). After performing the sums of the Matsubara frequencies, the thermodynamic potential Ω is written as

$$\Omega = \frac{1}{4G_1}\phi^2 + \frac{1}{4G_2}\Delta^2 - \sum_{\tau=u,d} \int \frac{p^2 dp}{\pi^2} \\ \times \Big\{ E_\tau + T\ln(1 + e^{-\beta(E_\tau - \mu_\tau)}) + T\ln(1 + e^{-\beta(E_\tau + \mu_\tau)}) $$

$$+ \sqrt{\zeta_{\tau+}^2 + \Delta^2} + \theta(\zeta_{\tau-})\sqrt{\zeta_{\tau-}^2 + \Delta^2} \\ + 2T\ln(1 + e^{-\beta\sqrt{\zeta_{\tau+}^2 + \Delta^2}}) \\ + 2T\ln(1 + e^{-\beta\theta(\zeta_{\tau-})\sqrt{\zeta_{\tau-}^2 + \Delta^2}}) \Big\} + B', \quad (6)$$

where $\zeta_{\tau\pm} = E_\tau \pm \mu_\tau$, $E_\tau = \sqrt{m_\tau^{*2} + p^2}$ with $m_\tau^* = m_{\tau 0} + \phi$ and $\theta(x)$ is a step function defined as

$$\theta(x) = \begin{cases} 1 & x > 0 \\ -1 & x < 0. \end{cases} \quad (7)$$

The quark condensate $\langle \bar{\psi}\psi \rangle$ is related to ϕ via $\phi = -2G_1\langle \bar{\psi}\psi \rangle$.

In the four fermion interaction, form factors are not included [5]. Following Ref. [6], we introduce a cutoff, Λ_q to regulate the above integral. After minimizing the thermodynamic potential with respect to ϕ and Δ, the following gap equations can be obtained:

$$m_\tau^* = m_{\tau 0} + 4G_1 \int \frac{m_\tau^* p^2 dp}{\pi^2 E_\tau} \left\{ 1 - n_F(E_\tau) - \bar{n}_F(E_\tau) \right.$$
$$+ \frac{\zeta_{\tau+}}{\sqrt{\zeta_{\tau+}^2 + \Delta_\tau^2}} [1 - 2n_d(\zeta_{\tau+})]$$
$$\left. + \frac{\theta(\zeta_{\tau-})\zeta_{\tau-}}{\sqrt{\zeta_{\tau-}^2 + \Delta_\tau^2}} [1 - 2\bar{n}_d(\zeta_{\tau-})] \right\}, \quad (8)$$

$$\Delta_\tau = 4G_2 \int \frac{p^2 dp}{\pi^2} \left\{ \frac{\Delta_\tau}{\sqrt{\zeta_{\tau+}^2 + \Delta_\tau^2}} [1 - 2n_d(\zeta_{\tau+})] \right.$$
$$\left. + \frac{\theta(\zeta_{\tau-})\Delta_\tau}{\sqrt{\zeta_{\tau-}^2 + \Delta_\tau^2}} [1 - 2\bar{n}_d(\zeta_{\tau-})] \right\}, \quad (9)$$

where $n_F(E_\tau)$ and $\bar{n}_F(E_\tau)$ are the quark and antiquark distributions, respectively, expressed as

$$n_F(E_\tau) = \{\exp[(E_\tau - \mu_\tau)/T] + 1\}^{-1}, \quad (10)$$
$$\bar{n}_F(E_\tau) = \{\exp[(E_\tau + \mu_\tau)/T] + 1\}^{-1}. \quad (11)$$

The function $n_d(\zeta_{\tau+})$ and $\bar{n}_d(\zeta_{\tau-})$ are defined as

$$n_d(\zeta_{\tau+}) = \left\{ \exp\left[\sqrt{\zeta_{\tau+}^2 + \Delta_\tau^2}/T\right] + 1 \right\}^{-1}, \quad (12)$$
$$\bar{n}_d(\zeta_{\tau-}) = \left\{ \exp\left[\theta(\zeta_{\tau-})\sqrt{\zeta_{\tau-}^2 + \Delta_\tau^2}/T\right] + 1 \right\}^{-1}. \quad (13)$$

From the thermodynamic potential Ω, the pressure and quark density can be obtained as $p_Q = -\Omega$ and $\rho_\tau = \partial\Omega/\partial\mu_\tau$. One can define baryon density as $\rho_N = \frac{1}{3}(\rho_u + \rho_d)$. In the chiral limit, the current quark mass $m_{u0} = m_{d0} = 0$. In this case, Eq. (8) has a trivial solution $m^* = 0$. The gap equation for Δ_q also has a trivial solution $\Delta = 0$. Therefore, for the massless quark, at some range of chemical potential or baryon density, there exist four sets of solutions: A. $m^* \neq 0$, $\Delta \neq 0$; B. $m^* \neq 0$, $\Delta = 0$; C. $m^* = 0$, $\Delta \neq 0$; D. $m^* = 0$, $\Delta = 0$. The system favors being in the phase with lowest thermodynamic potential. By comparing the thermodynamical potentials, one finds that the system will be in the phase with $m^* \neq 0$, $\Delta = 0$ at low chemical potential (temperature) and in the phase with $m^* = 0$ at large chemical potential (temperature). However, at low chemical potential (temperature), the system cannot be in the quark phase but in the hadronic phase. Therefore, we need to replace the EOS for chiral symmetry breaking quark matter by that for hadronic matter.

III. NUCLEAR MATTER

For hadronic matter it is possible to work from the quark level, as in the quark meson coupling model or even in the NJL model. However, in the NJL model it is essential to incorporate the effect of confinement (for example through proper time regularization) in order to avoid a chiral collapse [15]. In the

present work we adopt the more common hybrid approach and use the $SU(3)$ quark mean field model in the hadronic phase. In that model the total effective Lagrangian is written

$$\mathcal{L}_{\text{eff}} = \mathcal{L}_{q0} + \mathcal{L}_{qM} + \mathcal{L}_{\Sigma\Sigma} + \mathcal{L}_{VV} + \mathcal{L}_{\chi SB} + \mathcal{L}_{\Delta m_s}$$
$$+ \mathcal{L}_h + \mathcal{L}_c, \quad (14)$$

where $\mathcal{L}_{q0} = \bar{q}i\gamma^\mu \partial_\mu q$ is the free part for massless quarks. The quark-meson interaction $\mathcal{L}_{qM}$ can be written in a chiral $SU(3)$ invariant way as

$$\mathcal{L}_{qM} = g_s(\bar{\Psi}_L M \Psi_R + \bar{\Psi}_R M^+ \Psi_L)$$
$$- g_v(\bar{\Psi}_L \gamma^\mu l_\mu \Psi_L + \bar{\Psi}_R \gamma^\mu r_\mu \Psi_R)$$
$$= \frac{g_s}{\sqrt{2}} \bar{\Psi} \left(\sum_{a=0}^{8} s_a \lambda_a + i\gamma^5 \sum_{a=0}^{8} p_a \lambda_a \right) \Psi - \frac{g_v}{2\sqrt{2}} \bar{\Psi}$$
$$\times \left(\gamma^\mu \sum_{a=0}^{8} v_\mu^a \lambda_a - \gamma^\mu \gamma^5 \sum_{a=0}^{8} a_\mu^a \lambda_a \right) \Psi. \quad (15)$$

In the mean field approximation, the chiral-invariant scalar meson $\mathcal{L}_{\Sigma\Sigma}$ and vector meson $\mathcal{L}_{VV}$ self-interaction terms are written as

$$\mathcal{L}_{\Sigma\Sigma} = -\frac{1}{2} k_0 \chi^2 (\sigma^2 + \zeta^2) + k_1 (\sigma^2 + \zeta^2)^2$$
$$+ k_2 \left(\frac{\sigma^4}{2} + \zeta^4 \right) + k_3 \chi \sigma^2 \zeta - k_4 \chi^4 - \frac{1}{4}\chi^4$$
$$\times \ln \frac{\chi^4}{\chi_0^4} + \frac{\delta}{3} \chi^4 \ln \frac{\sigma^2 \zeta}{\sigma_0^2 \zeta_0}, \quad (16)$$

$$\mathcal{L}_{VV} = \frac{1}{2} \frac{\chi^2}{\chi_0^2} \left(m_\omega^2 \omega^2 + m_\rho^2 \rho^2 + m_\phi^2 \phi^2 \right)$$
$$+ g_4(\omega^4 + 6\omega^2 \rho^2 + \rho^4 + 2\phi^4), \quad (17)$$

where $\delta = 6/33$; σ_0, ζ_0 and χ_0 are the vacuum expectation values of the corresponding mean fields σ, ζ, and χ.

The Lagrangian $\mathcal{L}_{\chi SB}$ generates nonvanishing masses for the pseudoscalar mesons

$$\mathcal{L}_{\chi SB} = \frac{\chi^2}{\chi_0^2} \left[m_\pi^2 F_\pi \sigma + \left(\sqrt{2} m_K^2 F_K - \frac{m_\pi^2}{\sqrt{2}} F_\pi \right) \zeta \right], \quad (18)$$

leading to a nonvanishing divergence of the axial currents which in turn satisfy the partial conserved axial-vector current (PCAC) relations for π and K mesons. Pseudoscalar, scalar mesons and also the dilaton field χ obtain mass terms by spontaneous breaking of chiral symmetry in the Lagrangian (16). The masses of u, d, and s quarks are generated by the vacuum expectation values of the two scalar mesons σ and ζ.

In the quark mean field model, quarks are confined in baryons by the Lagrangian $\mathcal{L}_c = -\bar{\Psi} \chi_c \Psi$. $\chi_c(r)$ is a confinement potential, i.e., a static potential providing the confinement of quarks by meson mean-field configurations. In the numerical calculations, we choose $\chi_c(r) = \frac{1}{4}k_c r^2$, where $k_c = 1$ GeV fm^{-2}. The Dirac equation for a quark field Ψ_{ij} under the additional influence of the meson mean fields is

given by

$$[-i\vec{\alpha}\cdot\vec{\nabla} + \beta\chi_c(r) + \beta m_i^*]\Psi_{ij} = e_i^*\Psi_{ij}, \qquad (19)$$

where $\vec{\alpha} = \gamma^0\vec{\gamma}$, $\beta = \gamma^0$, the subscripts i and j denote the quark i ($i = u, d, s$) in a baryon of type j ($j = N, \Lambda, \Sigma, \Xi$). The quark mass m_i^* and energy e_i^* are defined as

$$m_i^* = -g_\sigma^i \sigma - g_\zeta^i \zeta + m_{i0} \qquad (20)$$

and

$$e_i^* = e_i - g_\omega^i \omega - g_\phi^i \phi, \qquad (21)$$

where e_i is the energy of the quark under the influence of the meson mean fields. The effective baryon mass can be written as

$$M_j^* = \sum_i n_{ij} e_i^* - E_j^0, \qquad (22)$$

where n_{ij} is the number of quarks with flavor "i" in a baryon j and E_j^0 is adjusted to give a best fit to the free baryon mass.

Based on the previously defined quark mean field model the Lagrangian density for nuclear matter is written as

$$\begin{aligned}
\mathcal{L} = &\; \bar{\psi}(i\gamma^\mu\partial_\mu - M_N^*)\psi + \tfrac{1}{2}\partial_\mu\sigma\partial^\mu\sigma + \tfrac{1}{2}\partial_\mu\zeta\partial^\mu\zeta \\
&+ \tfrac{1}{2}\partial_\mu\chi\partial^\mu\chi - \tfrac{1}{4}F_{\mu\nu}F^{\mu\nu} - \tfrac{1}{4}\rho_{\mu\nu}\rho^{\mu\nu} \\
&- g_\omega\bar{\psi}\gamma_\mu\psi\omega^\mu - g_\rho\bar{\psi}_B\gamma_\mu\tau_3\psi\rho^\mu + \mathcal{L}_M,
\end{aligned} \qquad (23)$$

where

$$F_{\mu\nu} = \partial_\mu\omega_\nu - \partial_\nu\omega_\mu \quad \text{and} \quad \rho_{\mu\nu} = \partial_\mu\rho_\nu - \partial_\nu\rho_\mu. \qquad (24)$$

The term $\mathcal{L}_M$ represents the interaction between mesons which includes the scalar meson self-interaction $\mathcal{L}_{\Sigma\Sigma}$, the vector meson self-interaction $\mathcal{L}_{VV}$ and the explicit chiral symmetry breaking term $\mathcal{L}_{\chi SB}$, all defined previously. The Lagrangian includes the scalar mesons σ, ζ and χ, and the vector mesons ω and ρ. The interactions between quarks and scalar mesons result in the effective nucleon mass M_N^*. The interactions between quarks and vector mesons generate the nucleon-vector meson interaction terms of Eq. (23). The corresponding vector coupling constants g_ω and g_ρ are baryon dependent and satisfy the $SU(3)$ relationship: $g_\rho^p = -g_\rho^n = \tfrac{1}{3}g_\omega^p = \tfrac{1}{3}g_\omega^n$.

At finite temperature and density, the thermodynamic potential is defined as

$$\begin{aligned}
\Omega = &-\frac{k_B T}{(2\pi)^3}\sum_{N=p,n}\int_0^\infty d^3\vec{k}\{\ln(1 + e^{-(E_N^*(k)-\nu_N)/k_B T}) \\
&+ \ln(1 + e^{-(E_N^*(k)+\nu_N)/k_B T})\} - \mathcal{L}_M,
\end{aligned} \qquad (25)$$

where $E_N^*(k) = \sqrt{M_N^{*2} + \vec{k}^2}$. The quantity ν_N is related to the usual chemical potential, μ_N, by $\nu_N = \mu_N - g_\omega^N\omega - g_\rho^N\rho$. The energy per unit volume and the pressure of the system are, respectively, $\varepsilon = \Omega - \frac{1}{T}\frac{\partial\Omega}{\partial T} + \nu_N\rho_N$ and $p_H = -\Omega$, where ρ_N is the baryon density.

The mean field equation for meson ϕ_i is obtained by the formula $\partial\Omega/\partial\phi_i = 0$. For example, the equations for σ, ζ are

deduced as

$$\begin{aligned}
&k_0\chi^2\sigma - 4k_1(\sigma^2 + \zeta^2)\sigma - 2k_2\sigma^3 - 2k_3\chi\sigma\zeta - \frac{2\delta}{3\sigma}\chi^4 \\
&+ \frac{\chi^2}{\chi_0^2}m_\pi^2 F_\pi - \left(\frac{\chi}{\chi_0}\right)^2 m_\omega\omega^2\frac{\partial m_\omega}{\partial\sigma} \\
&- \left(\frac{\chi}{\chi_0}\right)^2 m_\rho\rho^2\frac{\partial m_\rho}{\partial\sigma} + \frac{\partial M_N^*}{\partial\sigma}\langle\bar{\psi}\psi\rangle = 0,
\end{aligned} \qquad (26)$$

$$\begin{aligned}
&k_0\chi^2\zeta - 4k_1(\sigma^2 + \zeta^2)\zeta - 4k_2\zeta^3 - k_3\chi\sigma^2 - \frac{\delta}{3\zeta}\chi^4 \\
&+ \frac{\chi^2}{\chi_0^2}\left(\sqrt{2}m_k^2 F_k - \frac{1}{\sqrt{2}}m_\pi^2 F_\pi\right) = 0,
\end{aligned} \qquad (27)$$

where

$$\begin{aligned}
\langle\bar{\psi}\psi\rangle = &\; \frac{1}{\pi^2}\int_0^\infty dk\frac{k^2 M_N^*}{E^*(k)}[n_n(k) + \bar{n}_n(k) \\
&+ n_p(k) + \bar{n}_p(k)].
\end{aligned} \qquad (28)$$

In the above equation, $n_N(k)$ and $\bar{n}_N(k)$ are the nucleon and antinucleon distributions, respectively, expressed as

$$n_N(k) = \frac{1}{\exp[(E^*(k) - \nu_N)/k_B T] + 1} \qquad (29)$$

and

$$\bar{n}_N(k) = \frac{1}{\exp[(E^*(k) + \nu_N)/k_B T] + 1}(N = n, p). \quad (30)$$

In the vacuum, the thermodynamic potential can have another solution where $\sigma = 0, \zeta = 0$ and $\chi = 0$. The energy difference of these two kinds of vacua is

$$\begin{aligned}
\Delta E = &\; \mathcal{L}_M(\sigma = 0, \quad \zeta = 0, \quad \chi = 0) - \mathcal{L}_M(\sigma = \sigma_0, \\
&\zeta = \zeta_0, \quad \chi = \chi_0).
\end{aligned} \qquad (31)$$

It is interesting that the calculated value ΔE is close to the bag constant of quark matter. (The numerical values of ΔE are listed in Table II.)

In the same way, the equations for the vector mesons, ω and ρ, can be obtained:

$$\frac{\chi^2}{\chi_0^2}m_\omega^2\omega + 4g_4\omega^3 + 12g_4\omega\rho^2 = g_\omega^N(\rho_p + \rho_n), \qquad (32)$$

$$\frac{\chi^2}{\chi_0^2}m_\rho^2\rho + 4g_4\rho^3 + 12g_4\omega^2\rho = \frac{1}{3}g_\omega^N(\rho_p - \rho_n), \quad (33)$$

where ρ_p and ρ_n are the proton and neutron densities, expressed as

$$\rho_N = \frac{1}{\pi^2}\int_0^\infty dk k^2[n_q(k) - \bar{n}_q(k)](N = p, n). \qquad (34)$$

In nuclear matter, when the density is high, the volume of the nucleon is important. The nucleon cannot be treated as a point-like particle. The excluded volume effect has been considered in Ref. [25]. The key point is that the pressure of a system with excluded volume is the same as that of a point

particle system, $p_H(T, \tilde{\mu})$, if the chemical potentials of these two systems have the following relationship:

$$\mu = \tilde{\mu} + v_0 p_B(T, \tilde{\mu}), \qquad (35)$$

where v_0 is the volume of a nucleon. $p_B(T, \tilde{\mu})$ is the pressure generated by baryons, i.e., $p_B(T, \tilde{\mu}) = p_H - \mathcal{L}_M$. The baryon density, entropy density and the energy density of the system (without meson contribution) are given by the usual thermodynamic expressions. We find the following relations:

$$\rho_B = \left(\frac{\partial p_B}{\partial \mu}\right)_T = \left(\frac{\partial p_B}{\partial \tilde{\mu}}\right)_T \frac{\partial \tilde{\mu}}{\partial \mu} = \frac{\tilde{\rho}_B}{1 + v_0 \tilde{\rho}_B}, \qquad (36)$$

$$S_B = \left(\frac{\partial p_B}{\partial T}\right)_\mu = \left(\frac{\partial p_B}{\partial T}\right)_{\tilde{\mu}} + \left(\frac{\partial p_B}{\partial \tilde{\mu}}\right)_T \left(\frac{\partial \tilde{\mu}}{\partial T}\right)_\mu$$

$$= \frac{\tilde{S}_B}{1 + v_0 \tilde{\rho}_B}, \qquad (37)$$

$$\varepsilon_B = TS_B - p_B + \mu \rho_B = \frac{\tilde{\varepsilon}_B}{1 + v_0 \tilde{\rho}_B}. \qquad (38)$$

When the effect of the finite volume of the nucleon is included, the scalar density, $\langle \bar{\psi} \psi \rangle$, in Eq. (26) becomes

$$\langle \bar{\psi} \psi \rangle = \frac{1}{\pi^2 (1 + v_0 \tilde{\rho}_B)} \int_0^\infty dk \frac{k^2 M_N^*}{E^*(k)}$$

$$\times [n_n(k) + \bar{n}_n(k) + n_p(k) + \bar{n}_p(k)]. \qquad (39)$$

The phase transition from hadronic matter to quark matter is determined by the following conditions:

$$p_H = p_Q, \quad \mu_p = 2\mu_u + \mu_d, \quad \mu_n = \mu_u + 2\mu_d. \qquad (40)$$

We should mention that at finite temperature, gluons make an important contribution to the pressure of quark matter. The gluon contribution to the pressure of quark matter is expressed as

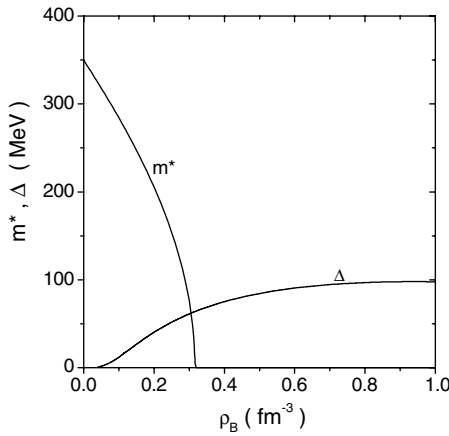$$p_g = \frac{8}{3\pi^2} \int_0^\infty dk \frac{k^3}{e^{k/k_B T} - 1}. \qquad (41)$$

FIG. 1. Effective quark mass and superconducting energy gap calculated in the NJL model versus baryon density at zero temperature.

TABLE I. Parameters of the $SU(3)$ quark mean field model.

R(fm)	k_0	k_1	k_2	k_3	k_4	g_s	g_v	g_4
0	3.97	2.18	−10.16	−4.15	−0.14	4.76	8.70	15.0
0.6	3.95	1.83	−10.16	−4.56	−0.10	4.76	8.70	15.0
0.75	3.94	1.40	−10.16	−5.13	−0.03	4.76	8.70	15.0

IV. NUMERICAL RESULTS

In the NJL model, Λ_q is chosen to obtain the quark condensate $\langle \bar{q}q \rangle = -250$ MeV. G_1 is determined by the bold quark mass in vacuum $m_q = 350$ MeV. There is some uncertainty in the coupling constant G_2. The instanton interaction suggests $G_2/G_1 = 1/2$, while in Ref. [5], this ratio is 3/4. In our calculations we choose $G_2/G_1 = 0.6$, which is close to that of Ref. [6]. The parameter B' is determined by choosing the bag constant of quark matter to be 209 MeV, i.e., $p_Q(m_q^* = 0, \mu_q = 0) = -(209\text{MeV})^4$. The numerical values of these three parameters are $\Lambda_q = 634.7$ MeV, $G_1 = 5.6$ GeV^{-2}, and $(B')^{1/4} = 605.7$ MeV. As for the nuclear matter phase, the parameters in the Lagrangian, which are shown in Table I, are determined by the saturation properties and the meson masses in vacuum. The corresponding nuclear matter properties and scalar meson masses are listed in Table II.

In Fig. 1 we plot the nonzero solutions for the effective quark mass and energy gap versus baryon density at zero temperature. From the figure, one can see that the effective quark mass decreases continuously to zero with the increasing density. The energy gap also changes continuously with the density. However, at low temperature, the effective quark mass cannot decrease to zero continuously, as shown in Fig. 1. The energy gap cannot change continuously either—there is a first order phase transition. We have mentioned in Sec. II that there are four kinds of solutions to Eqs. (8) and (9). At a given chemical potential the system will be in the phase with the lowest thermodynamic potential (highest pressure). In Fig. 2 we plot the pressure versus quark chemical potential for the four kinds of solutions at zero temperature. The solid, dashed, dotted, and dash-dotted lines are for $m^* = 0, \Delta = 0$ (phase D); $m^* = 0, \Delta \neq 0$ (phase C); $m^* \neq 0, \Delta \neq 0$ (phase A) and $m^* \neq 0, \Delta = 0$ (phase B), respectively. At small chemical potential, the system will be in the phase B: $\Delta = 0, m^* \neq 0$. At large chemical potential, the system will be in the phase C: $\Delta \neq 0, m^* = 0$. The phase transition takes place when the chemical potential is about 342 MeV. Because this chemical potential is smaller than the effective quark mass in phase B, the density of this phase is zero. The effective mass and the energy gap versus chemical potential are shown in

TABLE II. Nuclear matter properties and scalar meson masses in the $SU(3)$ quark mean field model.

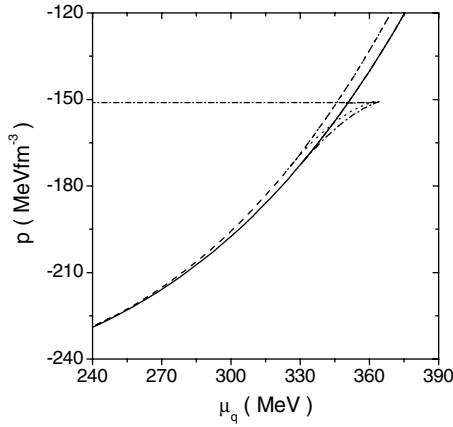| R (fm)	ρ_0 (fm^{-3})	E/A (MeV)	M_N^*/M_N	K (MeV)	$(\Delta E)^{1/4}$ (MeV)	m_σ (MeV)	m_ζ (MeV)
0	0.16	−16.0	0.742	303	220.2	487.8	1168.0
0.6	0.16	−16.0	0.731	359	215.5	490.0	1173.4
0.75	0.16	−16.0	0.713	473	209.5	491.6	1181.2

FIG. 2. Thermodynamic potential of quark matter versus quark chemical potential, μ_q, at zero temperature. The solid, dashed, dotted, and dash-dotted lines are for $m^* = 0$, $\Delta = 0$, $m^* = 0$, $\Delta \neq 0$, $m^* \neq 0$, $\Delta \neq 0$, and $m^* \neq 0$, $\Delta = 0$, respectively.

Fig. 3. At the transition point, $\mu_q = 342$ MeV, the changes in these quantities are discontinuous.

With increasing temperature the energy gap will decrease. Figure 4 shows the energy gap versus density at different temperatures. When the temperature is larger than about 52 MeV the Cooper pairs cannot form and the energy gap disappears. Figure 5 shows the corresponding phase diagram. The solid and dashed lines indicate first and second order phase transitions, respectively. At low temperature, the transition from phase B to phase C is of first order. The transition from phase C to phase D is second order. This means that the two p-μ curves, corresponding to phase C and D, turn into a single curve at the transition point. We should mention that the result of the second order phase transition is an artifact of the mean field approximation. Early in 1974, Halperin, Lubensky, and Ma showed that the superconducting to normal phase transition cannot be the second order [27]. In fact, this phase transition must be of the first order when gauge field fluctuation is included [28–31]. At high temperature the effective mass drops to zero continuously. The two p-μ curves of phase B
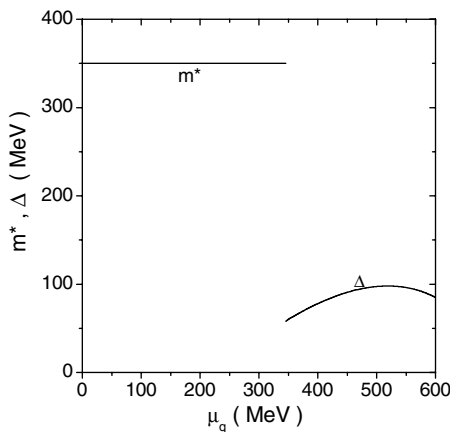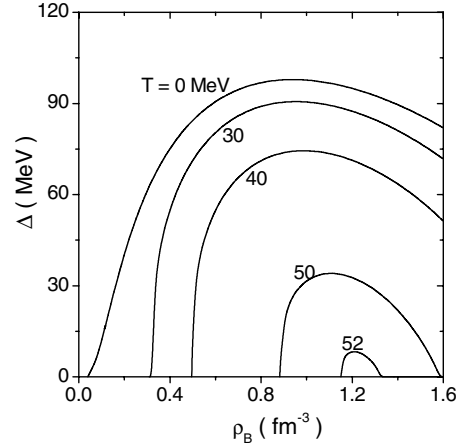

FIG. 4. Superconducting energy gap versus baryon density at different temperatures.

and D turn into one curve smoothly and they do not cross each other as at low temperature.

However, this phase diagram is for the transition from quark matter to quark matter, not for the transition from nuclear matter to quark matter. In nuclear matter the "elementary particles" are protons and neutrons. The equations of state for quark matter and nuclear matter are different. The energy per baryon for nuclear matter is shown in Fig. 6, where nucleon volume effects are considered. The three curves correspond to the nucleon radius $R = 0$, 0.6 fm and 0.75 fm, respectively. The inclusion of finite volume effects makes the EOS for nuclear matter harder and generates a strong repulsive interaction between nucleons.

The p-μ curves for nuclear matter and quark matter at zero temperature are shown in Fig. 7. The three solid curves are for nuclear matter and the two dashed lines for quark matter. If the nucleons are treated as point particles, there is no phase transition between nuclear matter and quark matter in this model. The chemical potentials for the nucleons are always
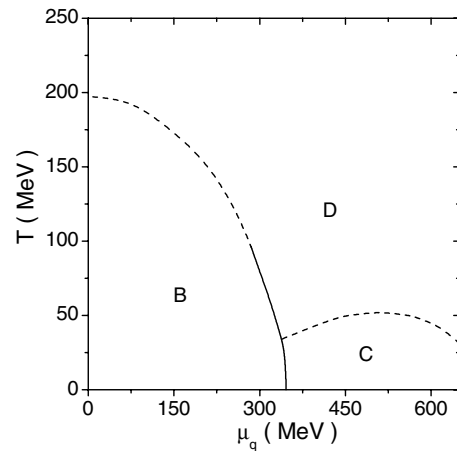

FIG. 3. Effective quark mass and superconducting energy gap versus quark chemical potential at zero temperature.

FIG. 5. T-μ phase diagram for quark matter. The solid line stands for the first order phase transition and dashed lines stand for the second order phase transition. B, C, and D correspond to the different phases explained in the text.
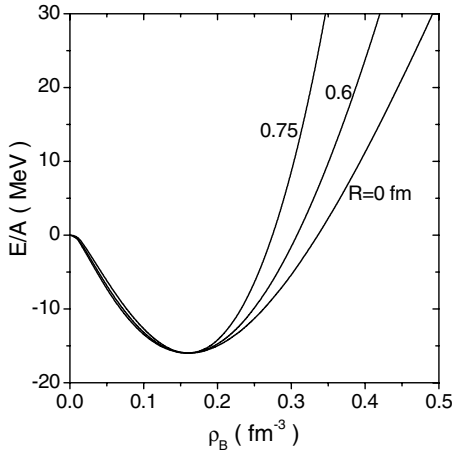
FIG. 6. The energy per baryon of nuclear matter versus baryon density. The radius of the nucleon is chosen to be 0, 0.6 fm and 0.75 fm, respectively.

smaller than the corresponding sums of quark potentials. When the volume effects are included, the nucleon chemical potentials will be increased and there is a first order phase transition between color superconducting quark matter and nuclear matter. The T-μ phase diagram for the transition between nuclear matter and quark matter is shown in Fig. 8. The solid and dashed lines indicate first and second order phase transitions, respectively. The letter H indicates the hadronic phase of nuclear matter. When the chemical potential is zero, the nuclear matter will turn into quark matter at temperature $T = 148$ MeV. At low temperature, the phase transition from nuclear matter to color superconducting quark matter will take place when the nucleon chemical potential, μ_N, is about 1.5–1.7 GeV.

Figures 9 and 10 show the T-ρ phase diagram for $R = 0.6$ fm and 0.75 fm, respectively. Since the phase transition is of first order, the densities of nuclear matter and quark matter are different. There is a coexistence state, M, in the figures. For the case of $R = 0.6$ fm, at zero temperature, when the nuclear density is about 0.76 fm^{-3}, quark matter starts to appear with

FIG. 8. T-μ phase diagram for nuclear matter and quark matter. The solid lines are for first order phase transition between nuclear matter and quark matter. The dashed line is for the second order phase transition between superconducting quark matter and normal quark matter. H is for the phase of nuclear matter and C and D are for the quark phases.

density around 1.17 fm^{-3}. For the case $R = 0.75$ fm, the corresponding densities of nuclear matter and quark matter are 0.44 fm^{-3} and 0.85 fm^{-3}. From our calculation, we conclude that at low temperature, when the nuclear density is of order $2.5\rho_0$–$5\rho_0$, where ρ_0 is the saturation density of symmetric nuclear matter, there will be a phase transition. Since the phase transition between color superconducting quark matter and normal quark matter is of second order, the density remains the same during the phase transition.

In our calculation, most parameters are fixed by well known physical quantities. Besides the nucleon radius R, there is only one parameter, the bag constant, which will sensitively affect the transition density and temperature. We discuss how the bag constant affects the transition temperature at zero baryon density. From Fig. 11, one can see that with increasing
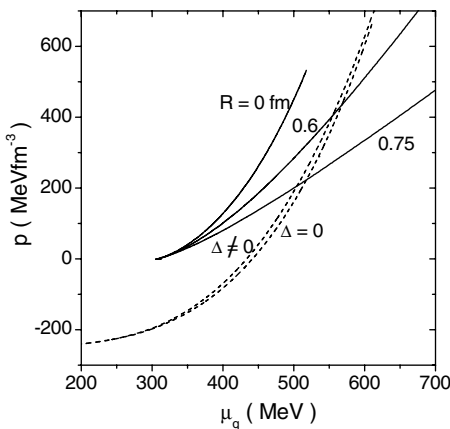

FIG. 7. Pressure of nuclear matter and quark matter versus chemical potential. The solid lines are for nuclear matter and dashed lines are for quark matter.
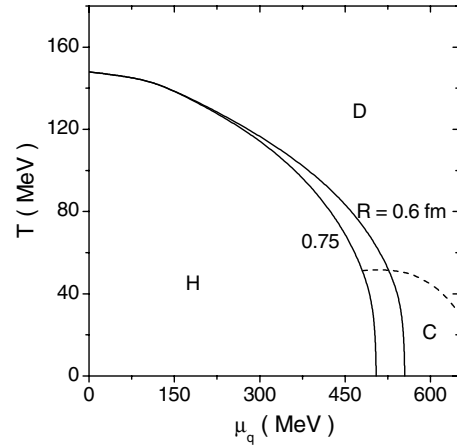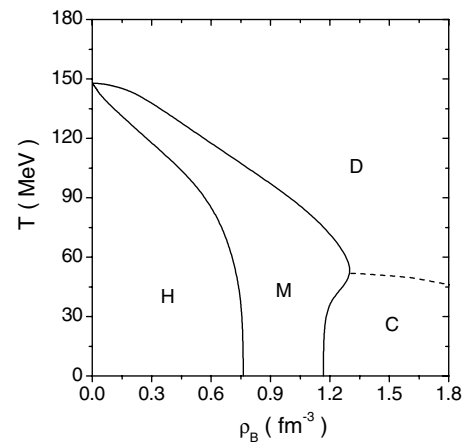

FIG. 9. T-ρ phase diagram for nuclear matter and quark matter. The radius of nucleon is chosen to be 0.6 fm. H is for the phase of nuclear matter. M is for the mixed phase. C and D are for the quark phases.
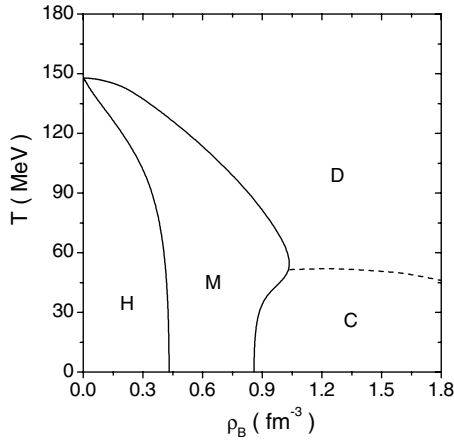
FIG. 10. T-ρ phase diagram for nuclear matter and quark matter. The radius of the nucleon is chosen to be 0.75 fm. H is for the phase of nuclear matter. M is for the mixed phase. C and D are for the quark phases.

temperature, the pressure of nuclear matter at zero baryon density increases very slowly. Until the temperature is around 180 MeV, the pressure remains low. However, for quark matter, the pressure increases very fast when the temperature is larger than about 90 MeV. This is because the quark mass is much smaller than the nucleon mass. If the bag constant lies in the range $180 < B^{1/4} < 230$ MeV, the transition temperature at zero baryon density is in the range $130 < T < 170$ MeV. In other words, if the transition temperature is about 150 MeV the bag constant will be around $(210\ \text{MeV})^4$ which means that our choice of bag constant is reasonable.

V. SUMMARY

We have investigated the phase transition from nuclear matter to quark matter. The $SU(3)$ quark mean field model, including nucleon volume effects, has been applied to get the
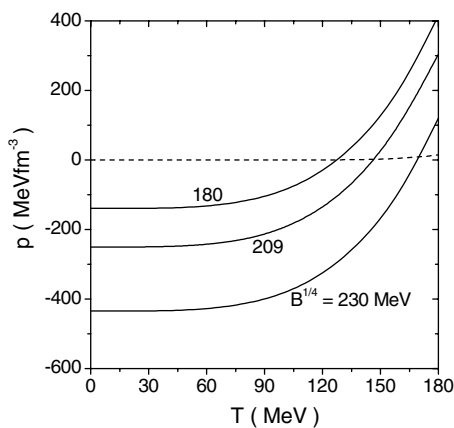

FIG. 11. Pressure of nuclear and quark matter at zero baryon density versus temperature. The solid lines are for quark matter with the different bag constants. The dashed line is for nuclear matter.

EOS of nuclear matter. Color superconducting quark matter has also been studied, using the NJL model. The parameters in the models are determined by well known physical quantities. We now summarize the main results.

The phase transition between nuclear matter and quark matter is of first order. There is no critical temperature above which the phase transition is of second order. The so-called second order phase transition is a transition from chiral symmetry breaking quark matter to chiral symmetry restored quark matter. However, in the real world, at low density or temperature, there is no chiral symmetry breaking quark matter, but rather one has nuclear matter. Therefore, the phase transition from nuclear matter to quark matter is always a first order transition, since the EOS of nuclear and quark matter are different.

The effects of the finite volume of the nucleon are very important, especially at high density. The volume effects generate a strong repulsive interaction between the nucleons and increase their chemical potentials. The transition density is sensitive to the nucleon radius. In our numerical calculations, we chose $R = 0.6$ fm and 0.75 fm. At low temperature, when the nuclear density is of order $2.5\rho_0$–$5\rho_0$, the color superconducting quark phase will appear with a density $0.4\ \text{fm}^{-3}$ larger than that of nuclear matter.

Besides the nucleon radius, the phase transition is also sensitive to the bag constant B. If the bag constant is in the range 180 MeV $< B^{1/4} < 240$ MeV, the transition temperature will be 130 MeV $< T < 170$ MeV. The bag constant B can be explained as the energy difference, ΔE, between two kinds of vacua. In the $SU(3)$ quark mean field model, the calculated ΔE is reasonable, giving a transition temperature around 150 MeV.

At low temperature, when the density increases, the nuclear matter will always turn into color superconducting quark matter. When the temperature is larger than about 52 MeV, the superconductivity phase disappears. The transition from normal quark matter to color superconducting quark matter is of second order, while the transition from nuclear matter to quark matter is of first order.

In conclusion, we note that our discussions concerning the order of the phase transitions investigated here have been based upon mean field theory. In fact, for the transition from superconducting quark matter to normal quark matter, with the gluon field fluctuation, this transition must be of the first order. It clearly will be important to explore such effects in the current model. In addition, we have presented results without any consideration of strangeness. As strange quarks may be expected to appear at perhaps 2.5 to 3 times normal nuclear matter density (for matter in beta equilibrium, as in a neutron star), it will also be of interest to extend the present model to include strange quarks.

[1] S. Lawley, W. Bentz, and A. W. Thomas, Phys. Lett. **B632**, 495 (2006); S. Lawley, W. Bentz, and A. W. Thomas, J. Phys. G **32**, 667 (2006).

[2] I. A. Shovkovy, nucl-th/0511014; Found. Phys. **35**, 1309 (2005).

[3] M. Alford, K. Rajagopal, and F. Wilczek, Nucl. Phys. **B537**, 443 (1999).

[4] N. O. Agasian, B. O. Kerbikov, and V. I. Shevchenko, Phys. Rep. **320**, 131 (1999).

[5] J. Berges and K. Rajagopal, Nucl. Phys. **B538**, 215 (1999).

[6] T. M. Schwarz, S. P. Klevansky, and G. Rapp, Phys. Rev. C **60**, 055205 (1999).

[7] R. J. Furnstahl, H. B. Tang, and B. D. Serot, Phys. Rev. C **52**, 1368 (1995).

[8] G. Carter, P. J. Ellis, and S. Rudaz, Nucl. Phys. **A603**, 367 (1996); Erratum-*ibid*. **A608**, 514 (1996).

[9] L. L. Zhang, H. Q. Song, P. Wang, and R. K. Su, Phys. Rev. C **59**, 3292 (1999).

[10] P. Papazoglou, S. Schramm, J. Schaffner-Bielich, H. Stöcker, and W. Greiner, Phys. Rev. C **57**, 2576 (1998).

[11] P. Papazoglou, D. Zschiesche, S. Schramm, J. Schaffner-Bielich, H. Stöcker, and W. Greiner, Phys. Rev. C, **59** 411 (1999).

[12] P. A. M. Guichon, Phys. Lett. **B200**, 235 (1988); S. Fleck, W. Bentz, K. Shimizu, and K. Yazaki, Nucl. Phys. **A510**, 731 (1990); K. Saito and A. W. Thomas, Phys. Lett. **B327**, 9 (1994); P. G. Blunden and G. A. Miller, Phys. Rev. C **54**, 359 (1996); H. Müller and B. K. Jennings, Nucl. Phys. **A640**, 55 (1998).

[13] K. Tsushima, K. Saito, J. Haidenbauer, and A. W. Thomas, Nucl. Phys. **A630**, 691 (1998); K. Tsushima, K. Saito, and A. W. Thomas, Phys. Lett. **B411**, 9 (1997); Erratum-*ibid*. **B421**, 413 (1998).

[14] A. W. Thomas, S. Theberge, and G. A. Miller, Phys. Rev. D **24**, 216 (1981); A. W. Thomas, Adv. Nucl. Phys. **13**, 1 (1984); G. A. Miller, A. W. Thomas, and S. Theberge, Phys. Lett. **B91**, 192 (1980).

[15] W. Bentz and A. W. Thomas, Nucl. Phys. **A696**, 138 (2001); W. Bentz, T. Horikawa, N. Ishii, and A. W. Thomas, *ibid*. **A720**, 95 (2003); H. Mineo, W. Bentz, N. Ishii, A. W. Thomas, and K. Yazaki, *ibid*. **A735**, 482 (2004) .

[16] H. Toki, U. Meyer, A. Faessler, and R. Brockmann, Phys. Rev. C **58**, 3749 (1998).

[17] P. Wang, Z. Y. Zhang, Y. W. Yu, R. K. Su, and H. Q. Song, Nucl. Phys. **A688**, 791 (2001).

[18] P. Wang, H. Guo, Z. Y. Zhang, Y. W. Yu, R. K. Su, and H. Q. Song, Nucl. Phys. **A705**, 455 (2002).

[19] Ping Wang, Zong-Ye Zhang, and You-Wen Yu, Commun. Theor. Phys. **36**, 71 (2001).

[20] P. Wang, V. E. Lyubovitskij, Th. Gutsche, and Amand Faessler, Phys. Rev. C **67**, 015210 (2003).

[21] P. Wang, D. B. Leinweber, A. W. Thomas, and A. G. Williams, Nucl. Phys. **A744**, 273 (2004).

[22] P. Wang, D. B. Leinweber, A. W. Thomas, and A. G. Williams, Phys. Rev. C **70**, 055204 (2004).

[23] P. Wang, D. B. Leinweber, A. W. Thomas, and A. G. Williams, Nucl. Phys. **A748**, 226 (2005).

[24] M. I. Gorenstein, V. K. Petrov, and G. M. Zinovjev, Phys. Lett. **B106**, 327 (1981).

[25] P. K. Panda, M. E. Bracco, M. Chiapparini, E. Conte, and G. Krein, Phys. Rev. C **65**, 065206 (2002).

[26] Y. Nambu and G. Jona-Lasinio, Phys. Rev. **122**, 345 (1961).

[27] B. I. Halperin, T. C. Lubensky, and S. Ma, Phys. Rev. Lett. **32**, 292 (1974).

[28] I. Giannakis, D. Hou, H.-c. Ren, and D. H. Rischke, Phys. Rev. Lett. **93**, 232301 (2004).

[29] I. Giannakis and H.-c. Ren, Nucl. Phys. **B669**, 462 (2003).

[30] T. Matsuura, K. Iida, T. Hatsuda, and G. Baym, Phys. Rev. D **69**, 074012 (2004).

[31] J. L. Noronha, H. C. Ren, I. Giannakis, D. F. Hou, and D. H. Rischke, Phys. Rev. D **73**, 094009 (2006).